OFSS

DEPARTMENT OF THE INTERIOR
UNITED STATES GEOLOGICAL SURVEY

TRACE-ELEMENT GEOCHEMISTRY OF POSTOROGENIC GRANITES FROM THE NORTHEASTERN ARABIAN SHIELD, KINGDOM OF SAUDI ARABIA

by

J. S. Stuckless, R. J. Knight, G. VanTrump, Jr.,

and J. R. Budahn

U.S. Geological Survey
Open-File Report 83-287

Prepared for:

Ministry of Petroleum and Mineral Resources
Deputy Ministry for Mineral Resources
Jiddan, Kingdom of Saudi Arabia
1402 AH 1982 AD

This report is preliminary and has not been reviewed for conformity with U.S. Geological Survey editorial standards.

1983

CONTENTS

ILLUSTRATIONS

TABLES

TRACE-ELEMENT GEOCHEMISTRY OF POSTOROGENIC GRANITES FROM THE NORTHEASTERN ARABIAN SHIELD, KINGDOM OF SAUDI ARABIA

by

J. S. Stuckless[1/], R. J. Knight[1/], G. VanTrump, Jr.[1/], and J. R. Budahn[1/]

ABSTRACT

Concentrations determined for all of the trace elements included in this study of postorogenic granites from the northeastern Arabian Shield are best described by log-normal distributions. The trace elements are divided into two groups: (1) compatible lithophile and siderophile elements (strontium, cobalt, scandium, manganese, europium, and titanium) and (2) incompatible lithophile elements (uranium, thorium, tantalum, rubidium, and rare-earth elements, except europium). The compatible elements exhibit greatest concentrations in the metaluminous postorogenic granites, and concentrations decrease with increasing degree of magma evolution. Economic potential for these elements and other geochemically similar elements is considered to be low. The concentrations of the incompatible elements increase with increasing degree of magma evolution and are greatest in the peralkaline and peraluminous granites. There is some geologic evidence that pegmatite and vein-forming processes were operative toward the end stage of postorogenic magmatism in the northeastern Arabian Shield, and therefore there is some probability for economic potential for these elements. It is suggested that such potential is greatest where highly evolved postorogenic granites intruded volatile (generally water)-rich country rocks.

1/ U.S. Geological Survey, Denver, Colorado 80225

INTRODUCTION

This report is the result of research performed by the U.S. Geological Survey (USGS) in accordance with a work agreement with the Ministry of Petroleum and Mineral Resources, Kingdom of Saudi Arabia. The research is part of a study of the petrogenesis and mineral potential of the granitic rocks of the Arabian Shield. This report will focus on the trace-element geochemistry of postorogenic granite samples described previously by Stuckless and others (unpub. data, 1982).

Postorogenic and anorogenic granites recently have received considerable attention because of their probable relationship to ore deposits (Wilson and Åkerblom, 1980; Doe and others, in press; Kinnaird and others, 1982) and because of their importance in the evolution of the continental crust (for example, Anderson and others, 1980; Anderson, in press). Many of these granites are highly evolved (for example, Barker and others, 1976; Anderson and Cullers, 1978; Cullers and others, 1981) and have anomalously high contents of incompatible trace elements (Harris and Marriner, 1980; Cole and others, 1981; Radain and others, 1981).

Elliott (unpub. data, 1982) has recognized two types of trace-element-enriched granites within the Arabian Shield of Saudi Arabia: (1) zirconium-niobium granites and (2) tin-tungsten granites. These two different types of trace-element enrichments may reflect two different source materials that have been identified isotopically by Stacey and others (1980) and J. S. Stacey and D. B. Stoeser (written commun., 1982). The latter authors interpret the two crustal source regions as dominantly oceanic and dominantly continental in affinities. Trace-element studies have proved highly useful in the identification of both source materials and magmatic processes (for example, Hanson, 1978). More recent studies of economic concentrations of trace elements have emphasized the role of water (Simpson and others, 1982; Watson and others, 1982) and other volatiles (Christiansen and others, in press). These studies suggest trace-element systematics that are consistent with high economic potential for anorogenic granites.

Classification of plutonic rocks in this report follows the recommendation of the IUGS Subcommission on the Systematics of Igneous Rocks (Streckeisen, 1973). The granites are subdivided on the basis of alumina saturation as defined by Shand (1951), such that rocks with molar ratios of $Al/(Na+K) < 1$ are peralkaline, $Al/(Na+K) > 1$ and $Al/(Na+K+Ca) < 1$ are metaluminous, and $Al/(Na+K+Ca) > 1$ are peraluminous. Sample locations and alumina saturations for samples are shown on figure 1.

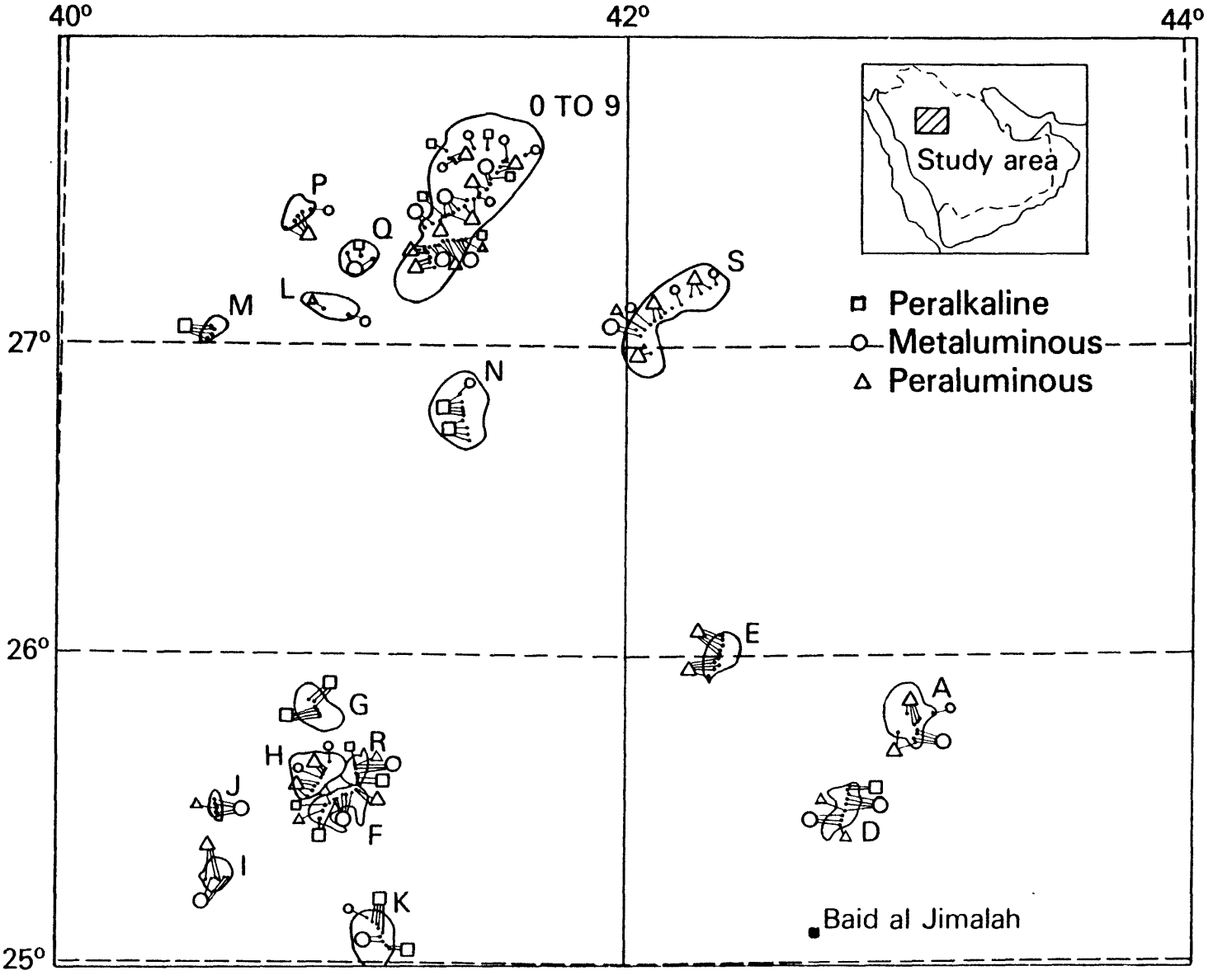

Figure 1.--Map showing sample locations and generalized outlines of postorogenic granites sampled from Stuckless and others(unpub data). Letter and numeric identifications are: A, Jabal Aban al Asmar; D, Jabal Aban al Ahmar; E, Jabal Qutn; F, Jabal Tuwalah; G, Jabal Awja; H, Ar Raqah; I, Jabal al Kurayziyah; J, Jabal Safad; K, Jabal Bidayah; L, Jabal ar Ra'ud; M, Bidat Nadhil; N, Jibal ar Rumman; P, Jibal Matali; Q, Jibal Kifantah; R, An Nammar, S, Jabal Salma; numbers 0 through 9, various phases of Jabal Aja.

ANALYTICAL PROCEDURES

Rubidium, strontium, and zirconium concentrations (table 1) were determined by X-ray fluorescence (XRF) for 10-g samples of unpacked powder of -200 mesh material. USGS standard rocks of granitic composition were used as monitors for data reduction. Comparison of rubidium and strontium results with those obtained by isotope dilution on a few of the samples (C. E. Hedge, written commun., 1982) suggests that the reported concentrations are precise and accurate to within ± 10 percent (2σ) for concentrations greater than 10 parts per million (ppm). Precision for zirconium values is estimated at ± 10 percent, but no independent check of accuracy has been made.

Trace-element concentrations reported in table 2 were determined by instrumental neutron activation analysis (INAA) on 1- to 2-g samples by use of methods similar to those described by Gordon and others (1968). Data were adjusted within the limits of counting statistics to yield smooth chondrite-normalized rare-earth-element patterns (Stuckless and Miesch, 1981). Chondrite values used for normalization are those reported by Evensen and others (1978). On the basis of the coefficient of variation in the counting statistics and analyses of standards, the accuracies of the values reported in table 2 are estimated to be ± 1 percent for tantalum, ± 2 percent for lanthanum, cerium, and neodymium, ± 3 percent for samarium, europium, ytterbium, scandium, and cobalt, ± 4 percent for terbium, hafnium, and antimony, ± 5 percent for dysprosium, lutetium, and cesium, ± 7 percent for thulium, and ± 14 percent for gadolinium.

Statistical evaluation of the data was accomplished by use of USGS RASS-STATPAC computer system (VanTrump and Meisch, 1977). Least-square fits to linear trends of data were made by use of the two error regression methods of York (1969).

RESULTS AND DISCUSSION

Trace-element concentrations and alumina saturation parameters are given in tables 1 and 2. Mathematical analyses of all trace-element data show that concentrations for each element are best approximated by a log-normal distribution. This relationship is indicated by the small absolute values for skewness and kurtosis for the logarithms of the concentrations (table 3). Because of the better fit to a log-normal distribution, concentration data for trace-element statistics are evaluated logarithmically (tables 3 through 9). Antilogs are reported in parts per million (ppm) for geometric means and deviations (tables 3 and 4).

Table 1.--*Alumina saturation and rubidium (Rb), strontium (Sr), and zirconium (Zr) concentrations for postorogenic granites from the northeastern Arabian Shield*

[Sample descriptions and locations in Stuckless and others, 1982. Rb, Sr, and Zr in parts per million]

Sample	Al/(Na+K)	Al/(Na+K+Ca)	Rb	Sr	Zr	Rb/Sr
155001	1.06	1.02	194	15.0	399	12.9
155002	1.25	1.06	217	101	132	2.14
155003	1.07	1.01	420	9.0	197	46.7
155004	1.08	1.02	306	11.4	177	26.8
155005	1.08	1.00	292	9.7	217	30.1
155006	1.08	0.95	114	44.1	568	2.58
155007	1.06	.98	170	23.1	238	7.35
155008	1.04	.98	142	18.5	259	7.67
155009	1.05	1.01	167	17.4	382	9.59
155010	1.07	.99	119	51.8	334	2.29
155011	1.04	.97	91.2	14.9	460	6.12
155012	1.07	.96	182	45.0	361	4.04
155016	1.05	.94	143	34.3	573	4.16
155013	1.19	1.06	142	122	93.0	1.16
155015	1.17	1.03	193	95.5	179	2.02
155017	1.30	1.13	171	58.7	67.6	2.91
155018	1.28	1.09	251	154	139	1.62
155019	0.95	.89	164	19.9	856	8.24
155020	.94	.89	181	24.5	792	7.38
155021	1.00	.92	140	29.1	435	4.81
155022	1.07	.98	145	105	413	1.38
155023	1.10	.97	134	98.2	406	1.36
155024	1.05	.98	150	77.7	85.4	1.93
155025	1.07	.98	167	53.6	328	3.11
155026	1.07	1.02	168	36.2	270	4.64
155027	1.06	.94	148	71.9	389	2.05
155028	1.07	.95	142	101	352	1.40
155029	1.08	1.03	133	44.0	247	3.02
155030	1.15	1.07	140	13.1	227	10.7
155031	1.13	1.03	188	28.9	220	6.50
155032	1.12	1.03	330	6.5	187	50.8
155033	1.16	1.08	308	29.9	174	10.3
155034	1.12	1.00	295	26.4	201	11.2
155035	1.18	1.06	221	52.0	182	4.25
155036	1.18	1.06	243	56.1	174	4.33
155037	1.17	1.05	267	49.7	196	5.37
155038	1.18	1.02	265	71.1	198	3.72
155039	1.11	1.02	408	4.8	212	85.0
155040	.98	.95	137	8.9	536	15.4
155041	1.04	1.01	141	6.6	498	21.4
155042	.95	.94	177	10.4	558	17.0
155043	1.06	1.00	160	15.2	1,150	10.5
155044	1.04	.96	182	15.8	880	11.5
155045	.97	.94	234	8.3	454	28.2
155046	.97	.94	201	10.4	498	19.3

Table 1.--*Alumina saturation and rubidium (Rb), strontium (Sr), and zirconium (Zr) concentrations for postorogenic granites from the northeastern Arabian Shield*--Continued

Sample	Al/(Na+K)	Al/(Na+K+Ca)	Rb	Sr	Zr	Rb/Sr
155047	1.02	0.93	154	41.6	440	3.70
155048	1.04	.97	212	26.4	988	8.03
155049	1.00	.94	161	25.8	551	6.24
155050	1.05	.98	192	10.8	1,020	17.8
155052	1.05	1.01	191	6.8	1,200	28.1
155053	1.06	1.02	261	16.9	955	15.4
155055	0.96	.89	144	16.3	1,010	8.83
155056	.96	.89	138	17.6	835	7.84
155057	1.01	.89	154	51.4	739	2.99
155058	1.05	.93	143	86.6	668	1.65
155059	1.08	.98	126	115	552	1.09
155060	1.15	1.07	137	21.5	665	6.37
155061	.98	.95	132	14.1	469	9.36
155062	.93	.87	235	16.1	2,080	14.6
155063	.87	.84	226	14.6	1,600	15.5
155064	.89	.87	213	6.4	1,080	33.3
155065	.90	.85	287	42.9	3,240	6.68
155066	.83	.81	364	4.9	587	74.3
155067	.99	.85	152	52.1	848	2.91
155068	.94	.92	196	6.3	349	31.1
155069	1.06	1.04	49.5	16.5	232	3.00
155070	1.06	1.00	52.5	24.4	238	2.15
155071	1.07	1.01	65.1	30.1	215	2.16
155072	1.09	1.08	77.7	16.1	421	4.82
155073	1.03	.97	76.8	28.8	392	2.66
155074	1.06	1.03	103	15.1	567	6.82
155075	1.09	1.01	101	28.5	688	3.54
155076	1.09	1.01	72.2	35.3	517	2.04
155077	1.06	.98	82.4	35.4	527	2.32
155078	1.10	1.02	94.2	49.4	299	1.90
155079	1.49	.82	42.3	590	317	0.07
155080	1.09	.92	60.3	66.9	516	.90
155081	1.20	1.06	94.7	167	152	.56
155082	1.17	1.02	105	162	169	.64
155083	1.03	.93	143	19.1	443	7.48
155084	1.08	.99	149	46.4	253	3.21
155085	1.24	.91	80.9	235	352	.38
155086	1.21	.90	101	209	357	.48
155087	1.08	.89	113	192	329	.58
155088	1.10	.94	126	151	277	.83
155089	1.03	1.00	123	37.5	667	3.28
155090	1.06	.87	101	114	423	.88
155091	.98	.92	90.6	34.5	298	2.62
155092	.99	.90	88.5	50.8	231	1.74
155093	1.01	.92	105	85.9	381	1.22

Table 1.--*Alumina saturation and rubidium (Rb), strontium (Sr), and zirconium (Zr) concentrations for postorogenic granites from the northeastern Arabian Shield*--Continued

Sample	Al/(Na+K)	Al/(Na+K+Ca)	Rb	Sr	Zr	Rb/Sr
155094	1.00	0.91	106	46.0	389	2.30
155095	0.96	.88	103	32.9	478	3.13
155096	.98	.92	98.3	38.4	282	2.55
155097	.99	.91	125	55.7	437	2.24
155098	.99	.91	109	63.3	393	1.72
155099	1.03	.98	94.4	21.4	499	4.41
155100	1.06	1.00	205	12.8	208	16.0
155101	1.11	1.04	232	8.9	348	26.1
155102	1.09	1.02	186	<1.0	265	>186
155103	1.13	1.02	208	9.8	332	21.2
155104	1.02	.97	247	11.8	321	20.9
155105	1.06	.99	201	24.0	255	8.37
155106	.85	.81	167	15.1	999	11.1
155107	1.08	1.04	198	9.4	452	21.1
155108	1.10	1.02	244	10.2	232	23.9
155109	1.03	.97	223	9.5	237	23.5
155110	1.11	1.03	207	13.1	307	15.8
155111	1.14	1.06	114	49.7	130	2.29
155112	1.10	1.01	154	60.1	336	2.56
155113	1.09	.98	60.7	115	485	0.52
155114	1.11	.96	61.2	128	716	.47
155115	1.10	1.04	182	13.7	308	13.3
155116	.90	.84	143	19.8	1,090	7.22
155117	1.04	.91	138	49.7	764	2.77
155118	1.10	1.01	183	26.9	260	6.80
155119	1.08	.99	228	14.3	345	15.9
155120	1.04	.96	226	19.1	422	11.8
155121	1.06	1.01	187	26.9	242	6.95
155122	1.05	.99	189	13.9	272	13.6
155123	1.07	1.03	195	19.0	308	10.3
155124	1.07	.99	180	11.5	200	15.7
155125	1.21	1.04	240	24.0	307	10.0
155126	1.20	1.03	190	156	159	1.21
155127	1.04	.99	144	58.3	196	2.46
155128	1.03	.99	189	26.0	286	7.26
155129	.96	.94	136	23.5	603	5.78
155130	1.08	1.02	185	22.1	216	8.37
155131	1.04	1.01	169	21.8	249	7.75
155132	1.10	1.02	140	26.7	290	5.24
155133	1.07	.99	171	20.6	345	8.30
155134	1.00	.95	144	24.6	373	5.85
155135	1.09	1.06	128	40.3	186	3.17
155136	.86	.83	173	10.4	627	16.6
155137	1.13	.98	118	61.7	689	1.91
155138	1.06	1.02	199	13.8	143	14.4

Table 1.--*Alumina saturation and rubidium (Rb), strontium (Sr), and zirconium (Zr) concentrations for postorogenic granites from the northeastern Arabian Shield*--Continued

Sample	Al/(Na+K)	Al/(Na+K+Ca)	Rb	Sr	Zr	Rb/Sr
155139	1.06	1.01	281	16.3	216	17.2
155140	1.01	0.95	143	21.7	285	6.58
155141	1.04	1.01	167	22.2	208	7.52
155142	0.94	.89	148	29.0	691	5.10
155143	.95	.89	159	27.2	1,140	5.84
155144	.96	.90	166	25.5	1,010	6.50
155145	.91	.84	122	22.8	440	5.35
155146	1.00	.97	110	16.9	836	6.50
155147	.98	.90	65.3	31.3	143	2.08
155148	.85	.79	125	24.9	828	5.02
155149	.89	.81	95.0	26.1	680	3.63
155150	.90	.83	93.9	36.1	733	2.60
155151	.97	.83	95.1	87.9	634	1.08
155152	.90	.86	132	38.0	1,430	3.47
155153	.96	.90	97.3	44.6	559	2.18
155154	.90	.85	117	20.2	580	5.79
155155	.90	.84	95.8	28.8	612	3.32
155156	1.08	.94	161	115	261	1.40
155157	1.10	.98	193	72.3	225	2.66
155158	1.02	.99	270	5.0	237	54.0
155159	.93	.85	153	24.9	859	6.14
155160	1.09	.98	83.3	40.2	291	2.07
155161	1.14	1.02	92.8	29.7	224	3.12
155162	1.17	1.07	91.8	44.6	219	2.05
155163	1.17	1.08	82.6	61.0	223	1.35
155164	1.10	1.00	101	39.0	182	2.58
155165	1.03	.95	100	17.1	485	5.84
155166	.97	.93	129	6.6	297	19.5
155167	1.01	.93	103	13.0	458	7.92
155168	1.07	1.00	216	5.9	170	36.6
155169	1.10	1.01	168	43.4	140	3.87
155170	1.05	.98	174	17.8	195	9.77
155171	1.08	.99	160	28.1	344	5.69
155172	1.13	1.02	156	60.1	218	2.59
155173	1.09	.99	159	88.6	223	1.79
155174	1.09	.98	171	69.3	229	2.46
155175	1.11	1.02	103	98.6	225	1.04
155176	1.08	1.01	232	10.7	168	21.7
155177	1.08	1.01	217	15.2	157	14.3
155178	1.10	1.03	181	29.8	138	6.07
155179	1.07	.98	182	23.1	167	7.87
155180	1.12	1.01	171	70.4	197	2.42
155181	1.08	1.00	191	55.2	234	3.46
155182	1.09	1.02	193	22.4	193	8.61
155183	1.17	.86	77.3	221.	861	0.34

Table 2.--*Quantitative trace-element data for granite samples from four postorogenic plutons from the northeastern Arabian Shield*

[Sample descriptions and locations in Stuckless and others, 1982. All results in parts per million. Leader (--) indicates no data. Chondrite-normalized rare-earth-element patterns plotted in figure 3 as indicated]

Sample	La ppm	Ce ppm	Nd ppm	Sm ppm	Eu ppm	Gd ppm	Tb ppm	Dy ppm	Tm ppm	Yb ppm	Lu ppm	Cs ppm	Ta ppm	Hf ppm	Sb ppm	Sc ppm	Co ppm	Remarks
Jabal Aban al Ahmar																		
Peralkaline samples																		
155019	73.8	173	81.5	17.3	0.765	17.3	2.93	18.2	1.46	8.67	1.21	2.07	7.08	23.9	1.07	0.50	0.213	Fig. 3c
155020	69.6	148	69.9	15.1	.698	14.8	2.44	15.3	1.29	7.75	1.13	3.48	5.57	20.0	2.02	.74	.317	Fig. 3c
Metaluminous samples																		
155021	56.5	127	56.7	12.3	.855	10.8	1.70	10.2	0.89	5.56	0.85	1.40	3.43	12.6	0.777	1.72	.482	Fig. 3b
155022	56.9	122	54.3	11.3	1.20	10.4	1.62	9.80	.84	5.19	.79	2.03	3.55	11.6	.793	3.55	1.09	Fig. 3b
155023	62.3	133	58.8	11.5	1.26	10.2	1.73	10.5	.92	5.55	.84	2.14	4.37	13.6	1.08	3.50	1.07	Fig. 3b
155024	32.6	68.9	33.9	6.92	.900	6.26	1.12	6.97	.54	3.09	.43	3.02	2.69	5.40	.623	1.62	.627	Fig. 3b
155025	58.1	125	52.8	11.2	.695	9.90	1.76	10.9	.97	5.96	.88	3.83	5.03	12.1	.539	1.63	.633	Fig. 3b
155027	58.4	123	51.9	10.5	.681	10.1	1.72	11.0	.95	5.86	.85	3.75	4.70	11.4	.565	1.57	.580	Fig. 3b
155028	52.1	109	48.8	10.2	1.18	9.07	1.50	9.19	.80	4.90	.74	4.15	3.82	10.9	.759	3.08	.894	Fig. 3b
Peraluminous samples																		
155026	46.0	100	44.6	9.53	.528	10.1	1.73	10.9	.97	5.69	.82	2.52	5.22	10.2	1.04	1.09	.424	Fig. 3d
155029	49.9	104	43.1	8.61	.836	7.57	1.16	6.92	.58	3.51	.53	1.42	2.89	7.82	.926	1.73	.602	Fig. 3d
Jabal Qutn																		
Peraluminous samples																		
155030	75.9	171	83.4	19.5	.393	21.6	3.67	23.8	1.99	12.0	1.70	1.77	3.10	8.49	.096	.40	.124	Fig. 3m
155031	53.1	117	51.9	11.5	.635	12.9	2.32	15.9	1.58	10.1	1.55	5.55	2.30	7.58	.366	.51	.253	Fig. 3m
155032	31.4	72.7	39.5	10.7	.171	13.9	2.63	18.6	2.37	16.3	2.66	9.66	6.80	7.98	.170	.96	.083	Fig. 3o
155033	28.7	67.2	32.6	8.50	.331	10.9	2.04	14.6	1.71	11.6	1.82	10.1	5.22	5.95	.149	1.68	.182	Fig. 3o
155034	34.9	79.3	40.6	10.9	.356	13.8	2.64	18.6	2.08	13.9	2.18	12.1	5.49	7.26	.229	1.68	.211	Fig. 3o
155035	27.3	63.5	30.1	7.37	.420	8.20	1.52	10.5	1.18	8.03	1.29	10.4	3.39	4.93	.131	3.39	.526	Fig. 3o
155036	24.8	56.5	29.0	7.36	.738	8.10	1.48	10.4	1.11	7.75	1.25	11.0	4.89	4.54	.202	3.30	.553	Fig. 3o
155037	31.6	76.6	37.8	9.91	.445	12.0	2.14	14.8	1.82	13.2	2.23	14.5	5.58	6.45	.288	2.34	.530	Fig. 3o
155038	31.4	75.9	36.3	9.77	.447	11.1	2.07	14.6	1.87	13.1	2.12	16.4	5.08	7.35	.609	3.03	.822	Fig. 3o
155039	41.1	88.3	38.8	10.5	.115	13.7	2.73	19.5	2.65	18.4	3.05	17.5	7.65	11.7	.974	.49	.138	Fig. 3o
Jabal Awja																		
Peralkaline samples																		
155062	79.2	184	89.6	19.4	.882	20.8	3.67	23.9	2.10	12.8	1.91	1.12	6.51	49.5	.243	.34	.125	Fig. 3n
155063	82.5	189	93.4	20.1	.878	20.5	3.52	22.1	1.91	11.2	1.65	1.24	5.72	32.6	.555	.31	.142	Fig. 3n
155064	61.1	131	75.4	17.5	.691	15.7	2.66	16.8	1.43	8.76	1.21	1.38	4.64	23.6	.207	.28	.111	Fig. 3n
155065	200	451	199	29.8	1.54	30.2	5.09	33.0	2.78	16.6	2.22	1.56	9.24	72.2	1.03	.89	.494	Fig. 3p
155066	20.3	47.8	26.8	6.59	.299	7.10	1.25	8.12	.72	4.49	.67	1.10	1.64	16.0	.113	.22	.263	Fig. 3p
155067	68.4	162	76.0	16.8	1.18	16.4	2.65	16.0	1.33	8.33	1.26	.66	4.28	23.7	.128	2.46	1.17	Fig. 3n
155068	16.5	38.7	23.9	6.60	.357	7.82	1.34	8.45	.72	4.49	.70	.80	1.58	9.73	.147	.33	.203	Fig. 3p

Table 2.--*Quantitative trace-element data for granite samples from four postorogenic plutons from the northeastern Arabian Shield*--Continued

Sample	La ppm	Ce ppm	Nd ppm	Sm ppm	Eu ppm	Gd ppm	Tb ppm	Dy ppm	Tm ppm	Yb ppm	Lu ppm	Cs ppm	Ta ppm	Hf ppm	Sb ppm	Sc ppm	Co ppm	Remarks
									Jabal Aja									
Peralkaline samples																		
155106	83.3	176	80.0	15.0	0.897	13.7	2.25	14.1	1.36	8.43	1.28	2.60	4.62	21.1	0.205	0.48	0.149	Fig. 3h
155116	102	232	103	20.5	1.25	20.3	3.31	20.1	1.65	9.31	1.35	0.89	6.23	24.5	.078	.45	.150	Fig. 3h
155129	79.1	177	87.2	15.7	1.06	13.7	2.03	12.0	.91	5.39	0.83	1.14	3.51	14.3	.087	.89	.323	Fig. 3h
155136	99.4	222	104	21.3	1.12	18.7	2.93	17.9	1.52	9.46	1.37	.84	4.77	14.5	.040	.33	.115	Fig. 3h
155159	121	265	121	23.2	1.57	21.6	3.35	19.4	1.53	9.28	1.41	.95	6.18	19.8	.115	1.13	.513	Fig. 3h
Peraluminous samples																		
155100	56.6	118	48.9	10.7	.246	9.91	1.78	11.4	1.07	6.46	0.94	1.78	6.62	12.2	.272	.48	.335	Fig. 3f
155101	64.1	138	55.0	11.8	.242	11.5	2.02	13.2	1.21	7.18	1.03	1.30	6.80	12.7	.213	.26	.240	Fig. 3f
155102	62.1	135	51.4	11.3	.240	10.6	1.88	11.7	1.13	6.77	.99	1.07	6.49	11.9	.165	.53	.312	Fig. 3f
155103	58.5	129	51.5	12.3	.149	12.2	2.22	14.8	1.42	8.75	1.27	1.78	8.91	15.5	.091	.21	.148	Fig. 3f
155107	56.5	109	48.7	11.2	.186	12.0	2.15	14.2	1.45	9.01	1.33	.80	6.57	15.7	.151	.32	.219	Fig. 3f
155108	85.4	170	64.7	13.1	.163	12.5	2.12	13.1	1.37	8.95	1.43	.95	6.15	---	.153	.39	.258	Fig. 3f
155110	57.4	129	53.6	12.8	.220	12.9	2.33	15.0	1.39	8.65	1.28	1.65	7.49	15.8	.147	.34	.169	Fig. 3f
155111	27.7	65.2	33.1	7.05	.607	6.88	1.11	7.00	0.64	4.09	0.64	2.01	0.52	5.95	.076	3.79	.960	Fig. 3e
155112	16.2	36.5	19.0	4.07	1.09	3.56	0.53	3.24	.30	1.93	.30	2.10	1.10	8.89	.129	2.14	.394	Fig. 3e
155115	55.7	121	54.3	11.8	.189	13.0	2.24	14.4	1.35	8.40	1.30	1.33	7.77	13.1	.121	.39	.196	Fig. 3f
155118	60.7	133	56.5	11.4	.288	10.9	1.93	12.3	1.12	6.93	1.03	1.59	6.32	12.0	.044	.72	.503	Fig. 3f
155121	62.5	127	55.5	11.8	.365	10.6	1.70	10.6	1.03	6.50	.97	2.27	6.13	11.9	.105	.57	.584	Fig. 3g
155123	73.0	158	66.7	13.5	.604	12.5	2.03	12.4	1.04	6.41	.94	1.14	5.80	13.3	.172	.75	.423	Fig. 3g
155125	50.1	107	47.1	10.8	.187	12.2	2.07	13.0	1.21	7.91	1.22	.87	7.69	12.9	.078	.48	.240	Fig. 3f
155126	37.6	75.2	31.2	5.60	.554	4.29	.71	4.73	.40	2.46	.36	4.99	2.19	6.33	.158	2.07	1.44	Fig. 3e
155130	56.3	118	49.9	9.61	.472	8.97	1.54	9.95	.84	5.30	.80	1.49	4.59	9.40	---	.62	.332	Fig. 3g
155131	58.3	122	50.7	9.85	.542	8.57	1.44	9.22	.87	5.40	.79	3.10	4.08	10.9	.130	.70	.464	Fig. 3g
155132	73.0	151	60.6	11.6	.778	9.20	1.49	8.93	.77	4.85	.73	.89	3.50	10.4	.128	.94	.514	Fig. 3g
155135	55.1	113	44.7	7.88	.771	6.04	.94	5.45	.45	2.69	.39	3.16	2.11	7.25	.267	1.00	.690	Fig. 3e
155138	43.5	92.4	37.1	7.68	.354	7.54	1.34	8.28	.76	4.59	.67	2.34	4.18	7.62	.424	.54	.310	Fig. 3g
155139	47.6	96.0	41.3	9.23	.373	9.25	1.68	11.3	1.24	8.24	1.25	6.95	11.8	13.3	.907	.80	.394	Fig. 3g
Metaluminous samples																		
155104	60.8	120	51.6	12.1	.139	11.9	2.16	14.5	1.49	9.24	1.44	2.55	9.22	16.1	.399	.24	.149	Fig. 3l
155105	55.4	113	46.9	10.5	.184	10.5	1.84	11.8	1.11	6.90	1.04	1.84	7.97	11.6	.356	.37	.207	Fig. 3l
155109	52.0	110	46.3	10.4	.181	10.5	1.73	10.9	1.11	7.07	1.08	1.92	6.20	12.2	.137	.32	.198	Fig. 3l
155113	61.9	140	64.8	10.7	2.13	8.20	1.16	6.20	.48	2.95	.44	1.07	1.19	11.9	.086	4.09	1.17	Fig. 3i
155114	59.8	132	60.0	9.98	1.89	7.63	1.11	5.80	.48	2.94	.44	1.39	1.17	16.7	.085	4.86	1.74	Fig. 3i
155117	84.1	183	90.1	18.0	1.90	16.9	2.67	15.5	1.28	7.61	1.13	1.02	4.52	19.0	.123	3.83	.448	Fig. 3i
155119	57.9	122	47.0	11.0	.185	11.3	1.95	13.0	1.34	8.84	1.37	1.18	9.24	16.7	.210	.31	.256	Fig. 3l
155120	97.3	200	80.9	15.6	.351	14.4	2.36	14.9	1.46	9.08	1.36	1.67	9.57	18.4	.187	.63	.331	Fig. 3l
155122	57.8	124	52.8	10.5	.413	9.85	1.62	10.0	.92	5.72	.85	2.14	3.79	11.5	.228	.47	.343	Fig. 3k
155124	47.6	97.0	45.2	10.3	.240	11.2	1.90	11.7	1.13	7.07	1.06	1.42	4.66	9.82	.189	.64	.260	Fig. 3l
155127	43.4	89.7	42.0	8.58	.429	8.28	1.21	6.91	.48	2.92	.43	1.99	1.73	9.04	.135	.99	.750	Fig. 3k
155128	61.6	129	58.4	11.4	.516	11.3	1.84	11.4	1.02	6.17	.90	2.77	4.90	12.4	.197	.64	.439	Fig. 3k
155133	68.6	144	59.5	12.1	.660	10.1	1.72	10.9	.96	6.06	.90	1.42	4.44	12.9	.113	.86	.600	Fig. 3j
155134	70.1	149	61.4	12.9	.694	10.9	1.89	12.0	1.09	6.65	.97	1.06	4.69	14.0	.051	1.07	.621	Fig. 3j
155137	89.8	189	89.2	16.5	2.10	14.3	2.30	13.1	1.03	6.27	.95	1.60	3.33	16.4	.136	6.23	.768	Fig. 3i
155156	60.5	123	50.0	9.37	.923	7.48	1.26	7.63	.66	4.14	.63	2.41	2.61	8.64	.080	2.34	1.98	Fig. 3j
155157	45.8	98.4	43.4	8.69	.681	7.29	1.30	8.08	.76	4.70	.71	3.40	2.73	7.52	.195	1.98	1.34	Fig. 3j
155158	31.7	76.7	41.1	10.7	.154	12.1	1.97	12.1	.87	5.09	.72	4.87	4.08	10.6	.242	.13	1.18	Fig. 3l

Table 3.--*Statistical analysis of trace-element concentrations for postorogenic granites from the northeastern Arabian Shield*
[Data evaluated logarithmically. Less-than or greater-than values not used for statistical calculation]

	Number of samples	Minimum (ppm)	Maximum (ppm)	Mean (ppm)	+σ (ppm)	-σ (ppm)	Skewness	Kurtosis
Rb	176	42.3	420	148	75	-50	-0.30	0.26
Sr	176	<1	590	29.2	41.0	-17.0	.40	.15
Zr	176	85.4	3240	370	317	-171	.53	.09
La	72	16.2	200	54.3	29.6	-19.1	-.45	1.40
Ce	72	36.5	451	118	61.8	-40.5	-.20	1.49
Nd	72	19.0	199	53.2	25.5	-17.2	.37	1.28
Sm	72	4.07	29.8	11.4	4.63	-3.29	.11	.96
Eu	72	0.115	2.13	0.513	0.565	-0.269	-.89	-.84
Gd	72	3.56	30.2	11.0	4.85	-3.37	-.15	1.25
Tb	72	.53	5.09	1.87	.86	-.59	-.39	1.43
Dy	72	3.24	33.0	11.8	5.75	-3.86	-.44	1.10
Tm	72	.30	2.78	1.08	.61	-.39	-.43	.35
Yb	72	1.93	18.4	6.73	3.94	-2.49	-.33	.22
Lu	72	.30	3.05	1.01	.61	-.38	-.24	.23
Cs	72	.66	17.5	2.19	2.67	-1.20	1.02	.42
Ta	72	.52	11.8	5.00	2.29	-2.29	.40	.18
Hf	71	4.54	72.2	12.2	7.69	-4.72	.83	2.16
Sb	71	.040	2.02	.218	.305	-.127	.54	-.38
Sc	72	.13	6.23	.87	1.29	-.52	.28	-.87
Co	72	.083	1.98	.382	.418	-.200	.14	-.66
Rb/Sr	176	.07	>186	5.07	10.8	3.45	-.28	.58
K/Rb	176	88	786	373	191	-126	.09	.14

Although the systematics of trace elements within a given suite of granitic rocks are dependent on a number of variables, trace-element data for the postorogenic granites of the northeastern Arabian Shield are similar in range and mean values to data for many postorogenic and anorogenic granites of North America (Buma and others, 1971; Barker and others, 1976; Anderson and Cullers, 1978; Anderson and others, 1980; Taylor and Strong, 1980; Cullers and others, 1981; Stuckless and Miesch, 1981). The North American examples range in age from Archean to Jurassic, but all exhibit features of highly evolved magma (that is, a magma derived by extensive fractional crystallization or by a low degree of partial melting). These features include high concentrations of one or more suites of incompatible trace elements, a fairly limited range in major-element composition, and strongly negative europium anomalies for at least some of the samples.

Several variables have been proposed or identified to explain observed trace-element systematics. The concentrations of some incompatible chalcophile elements, such as zinc, are largely controlled by province or protolith chemistry (for example, Bowden and Kinnaird, 1978). The concentrations of most incompatible lithophile elements, such as lithium, rubidium, cesium, beryllium, strontium, barium, scandium, rare-earth elements (REE), zirconium, hafnium, uranium, thorium, tantalum, and chromium, appear to be controlled by solidus-phase assemblages in the residuum left from partial melting or in that removed by fractional crystallization (for example, Hanson, 1978). The mineral assemblages reflect physical conditions during solid-liquid equilibration. For example, crystallization at high pressure may cause garnet to be a stable phase with consequent heavy REE (HREE) depletion in the liquid (for example, Arth and Hanson, 1972).

The composition of the volatile phase and degree of volatile saturation are important in the control of certain trace-element enrichments or depletions. High oxygen fugacity (greater than nickel-nickel oxide buffer) can stabilize epidote and allanite in metaluminous and peraluminous liquids as solidus phases in granitic magmas (Naney and Swanson, 1980) with consequent light REE (LREE) depletion (for example, Christiansen and others, in press). High oxygen fugacity may also partially suppress europium anomalies that develop by feldspar-magma equilibration (Sun and Hanson, 1976).

Christiansen and others (in press) have suggested that volatile transfer and complexing of trace elements with the volatile phase may lead to enrichments of lithium, rubidium, cesium, tantalum, thorium, beryllium, and HREE in fluorine-dominated systems. Volatile-phase transfer may also be important in the formation of peralkaline magma in which zirconium complexes with alkali elements. This complexing suppresses

zircon crystallization (Watson, 1979), and leads to enrichment of zirconium, hafnium, and HREE (for example, Buma and others, 1971). In addition, the peralkaline condition suppresses the crystallization of allanite and epidote, which in turn leads to LREE enrichment in the liquid.

Means and standard deviations for the trace-element concentrations in the postorogenic granites of the northeastern Arabian Shield subdivided by degree of alumina saturation are given in table 4. The differences in concentrations for most trace elements appear to be a function of alumina saturation. As predicted above, the peralkaline (alumina undersaturated) granites have the highest concentrations of zirconium, hafnium, and HREE. The relationship between zirconium concentration and alumina saturation is presented in figure 2. In comparison to the experimental data of Watson (1979), nearly all of the samples contain much more zirconium than would liquids of similar composition that were in equilibrium with zircon. Part of the increased zirconium content may be due to the differences between the chemically simple experimental system and a complex real system, such that synergistic effects of elements not included in the experimental system increase the zirconium saturation limit. In fact, the left boundary of the data field approximately parallels the experimental saturation limit. Nonetheless, most samples are enriched in zirconium by more than 100 percent; therefore, in a trace-element context, these samples probably do not represent equilibrium liquids.

Most surprising are the alumina-saturated and oversaturated samples, which are enriched in zirconium by approximately a factor of 10 relative to experimental equilibrium liquids. Such excess zirconium contents suggest loss of alkali elements, gain of aluminum, or gain of zirconium. Zirconium gain might be accomplished by addition of zircon crystallized elsewhere and assimilated by the magma or through volatile transfer. Although experimental evidence for volatile transfer of zirconium seems to be lacking, the existence of zircon-rich apophyses (Stuckless and others, unpub data) suggests that such a mechanism may exist.

Table 4 shows that there are differences in average REE contents, as a function of degree of alumina saturation; however, for the most part, the differences are not large as can be seen in a chondrite-normalized REE plot of the average data (fig. 3a). Relative to the metaluminous granites, the average peralkaline granite is enriched in all REE and has a slightly more negative europium anomaly. The average peraluminous granite is depleted in LREE, enriched in HREE, and has a more negative europium anomaly. The large negative europium anomalies suggest that the peraluminous and peralkaline granites represent the most evolved magma and that feldspar was a major crystalline phase during magma evolution (Hanson, 1978).

Table 4.--*Means and standard deviations for trace-element contents and ratios grouped by degree of alumina saturation*
[Data evaluated logarithmically; N is number of samples]

	Peraluminous			Metaluminous			Peralkaline		
	N	Mean (ppm)	σ (ppm)	N	Mean (ppm)	σ (ppm)	N	Mean (ppm)	σ (ppm)
Rb	70	166	+96 -61	65	135	+60 -42	41	142	+60 -42
Sr	69	24.9	+31.3 -13.9	65	41.7	+64.8 -25.4	41	21.5	+21.3 -10.7
Zr	70	258	+166 -101	65	381	+227 -142	41	651	+523 -290
La	33	46.5	+21.4 -14.7	25	57.5	+16.8 -13.0	14	70.6	+63.9 -33.5
Ce	33	101.	+42.0 -29.7	25	122.	+34.3 -26.8	14	159.	+140. -74.4
Nd	33	44.6	+14.9 -11.2	25	54.0	+14.0 -11.2	14	78.1	+56.5 -32.8
Sm	33	9.91	+3.23 -2.44	25	11.1	+2.48 -2.03	14	16.3	+8.63 -5.64
Eu	33	0.365	+0.282 -0.159	25	0.602	+0.811 -0.345	14	0.857	+0.535 -0.392
Gd	33	10.0	+4.17 -2.94	25	10.2	+2.58 -2.06	14	16.0	+7.54 -5.13
Tb	33	1.74	+0.83 -0.56	25	1.68	+0.45 -0.35	14	2.65	+1.22 -0.84
Dy	33	11.4	+5.87 -3.87	25	10.3	+3.14 -2.40	14	16.4	+7.58 -5.19
Tm	33	1.12	+0.72 -0.44	25	.90	+0.35 -0.25	14	1.39	+0.64 -0.44
Yb	33	7.10	+4.92 -2.91	25	5.53	+2.23 -1.59	14	8.40	+3.72 -2.58
Lu	33	1.08	+0.79 -0.46	25	.83	+0.35 -0.24	14	1.23	+0.50 -0.36
Cs	33	2.92	+4.82 -1.82	25	2.03	+1.16 -0.74	14	1.26	+0.76 -0.47
Ta	33	5.29	±2.37	25	4.55	±2.33	14	5.11	±2.04
Hf	32	9.38	+3.85 -2.73	25	12.1	+3.98 -2.99	14	22.8	+15.2 -9.11
Sb	32	.201	+0.244 -0.110	25	.237	+0.313 -0.135	14	.225	+0.477 -0.153
Sc	33	.340	+1.05 -0.47	25	1.19	+2.21 -0.77	14	.53	+0.50 -0.26
Co	33	.340	+0.299 -0.159	25	.584	+0.589 -0.293	14	.237	+0.233 -0.118
Rb/Sr	69	6.65	+12.8 -4.37	65	3.22	+7.36 -2.24	41	6.60	+10.4 -4.03
K/Rb	70	418	+235 -150	65	338	+144 -103	41	363	+169 -116

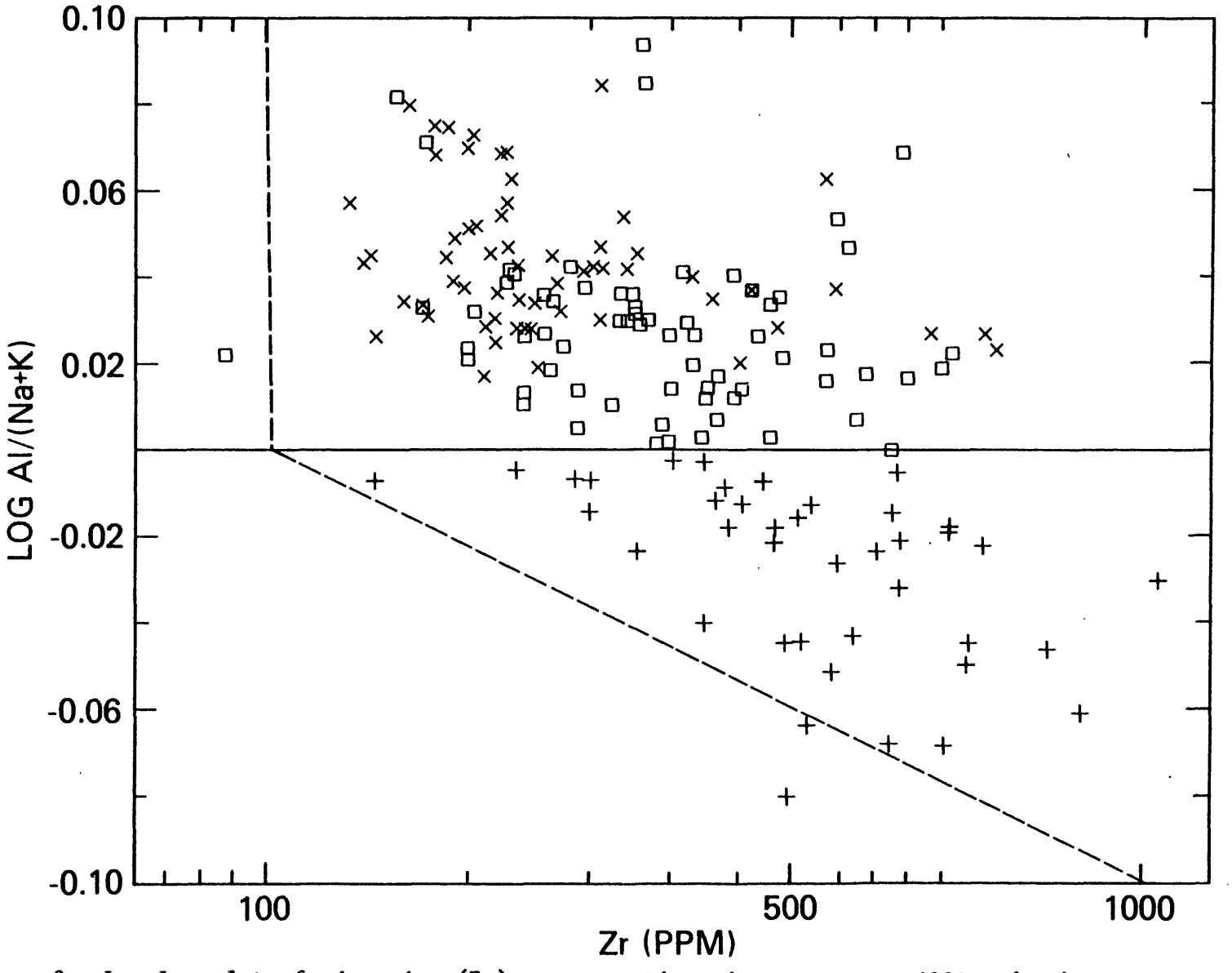

Figure 2.--Log-log plot of zirconium (Zr) concentrations in parts per million (ppm) versus molar Al/(Na+K) for postorogenic granites from the northeastern Arabian Shield. The solid horizontal line separates alumina-undersaturated granites (below) from alumina-saturated and oversaturated granites (above). The dashed line is the experimentally determined zirconium-saturation limit of Watson (1979). Symbols are: X, peraluminous granites; square, metaluminous granites; plus, peralkaline granites.

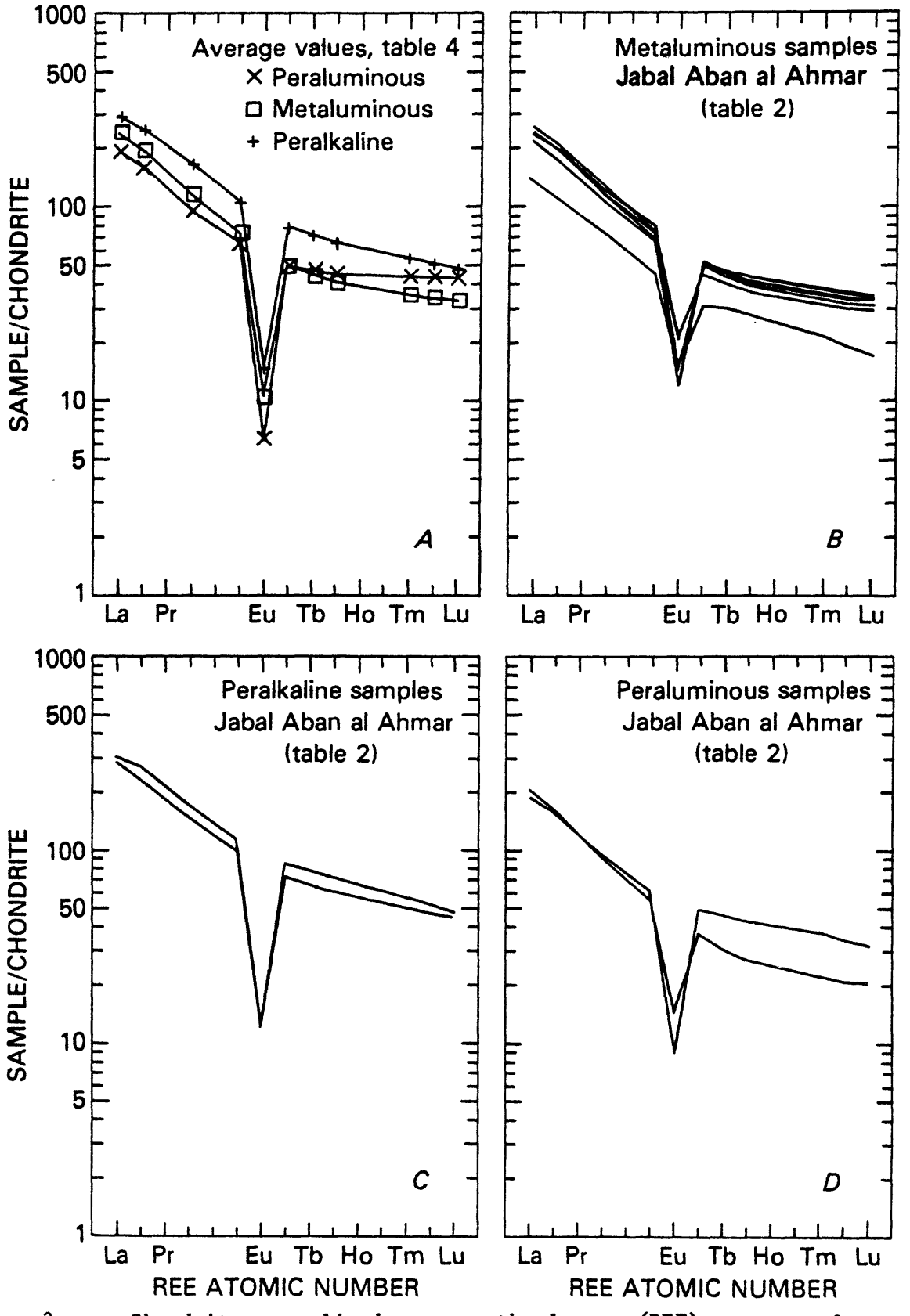

Figure 3a-p.--Chondrite-normalized rare-earth-element (REE) patterns for postorogenic granites from the northeastern Arabian Shield.

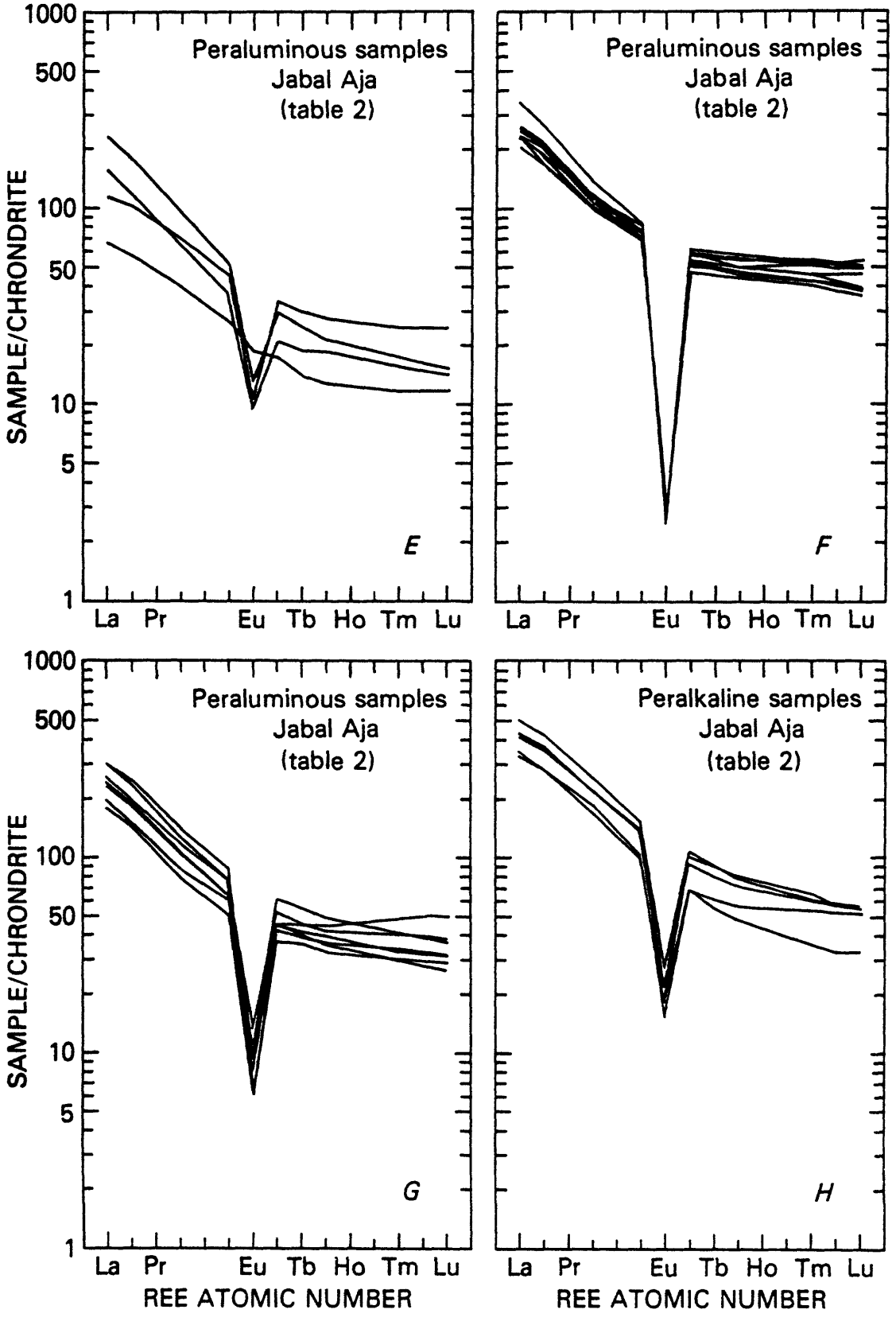

Figure 3a-p.--Continued

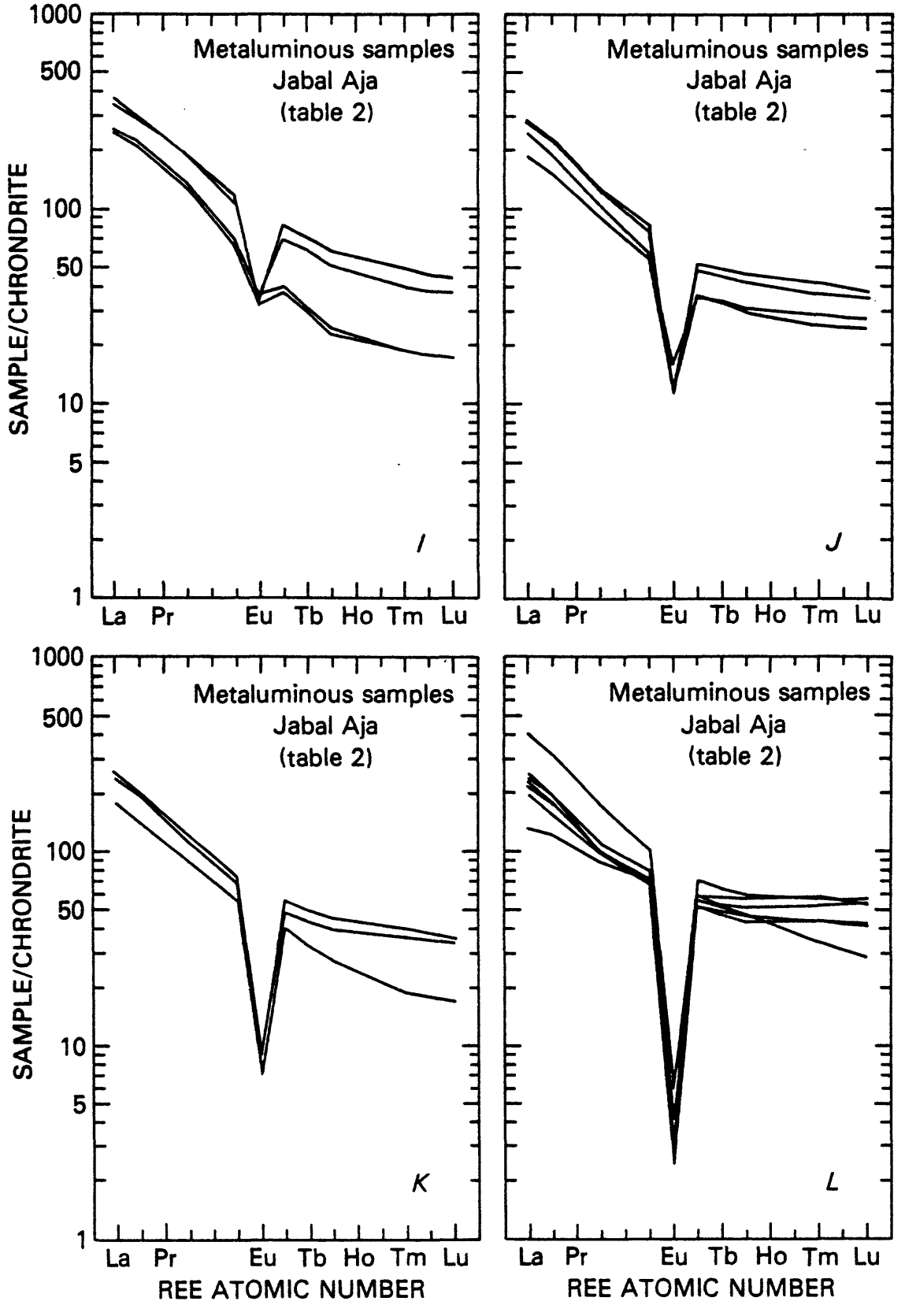

Figure 3a-p.--Continued

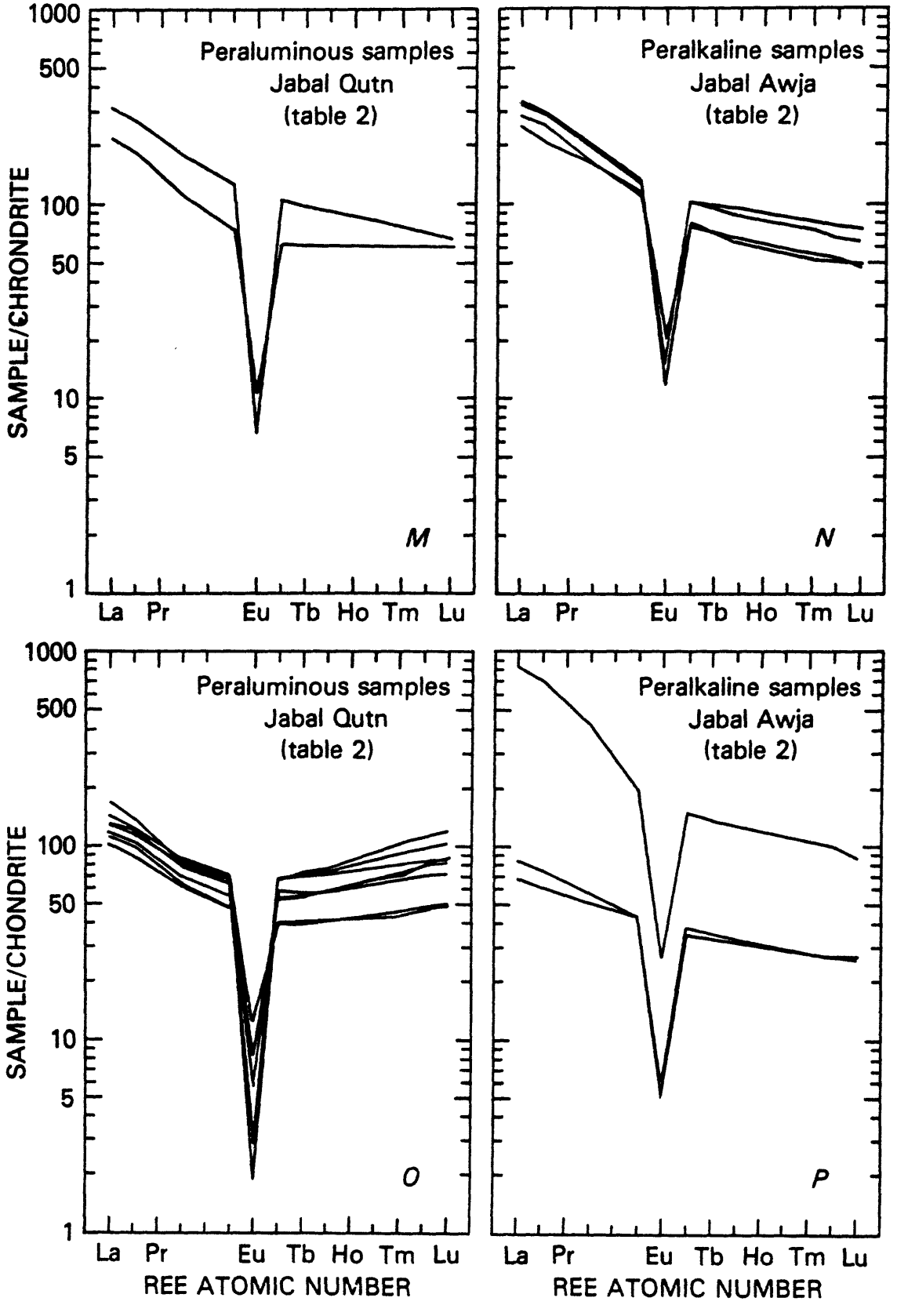

Figure 3a-p.--Continued

Differences among REE patterns are small even in single plutons that exhibit all three degrees of alumina saturation. REE patterns for metaluminous and peraluminous samples from Jabal Aban al Ahmar overlap completely (figs. 3b,d), and peralkaline samples are slightly enriched in REE (fig. 3c). Samples from Jabal Aja yield a wide variety of REE patterns (figs. 3e to l), but large, moderate, and small europium anomalies are noted for both peraluminous (figs. 3e,f,g,) and metaluminous (figs. 3j,k,l) granites. REE patterns for some metaluminous rocks (fig. 3i) overlap with those of peralkaline rocks (fig. 3h).

Even samples from plutons that exhibit only a single degree of alumina saturation yield REE patterns that overlap with those from plutons that have a different degree of alumina saturation. Some samples from Jabal Qutn (figs. 3m,o), which is entirely peraluminous, have REE patterns that overlap with those for samples from Jabal Awja (figs. 3n,p), which is entirely peralkaline. However, several samples from Jabal Qutn are distinct in that these are the only samples with relatively flat REE patterns (fig. 3o). By comparison to the steeper patterns from the same pluton, these may represent both LREE depletion and HREE enrichment.

The REE patterns for the postorogenic granites of the northeastern Arabian Shield are not only similar to one another for different plutons and for different degrees of alumina saturation but are also similar to those of other postorogenic and anorogenic granites that lack peralkaline components (Anderson and Cullers, 1978; Cullers and others, 1981; Stuckless and Miesch, 1981). The similar features, such as fairly flat REE patterns, chondrite-normalized LREE abundances from 100 to 300, and strongly negative europium anomalies for most samples, contrast with REE distributions noted for orogenic granites (Arth and Hanson, 1972, 1975; Frey and others, 1978). Orogenic granites typically exhibit much steeper REE patterns, chondrite-normalized LREE abundances of less than 100, and small or no europium anomalies. These differences reflect the much more highly evolved nature of postorogenic granites and the greater potential for economic concentrations of trace metals.

Further evidence of evolved magma and the direction of evolution is provided by the rubidium-strontium data. Bulk partition coefficients for rubidium in granitic magmas are generally less than one (Hanson, 1978). Conversely, bulk partitioning coefficients for strontium are generally greater than one (Hanson, 1978). Thus, with increasing degree of magma evolution, strontium concentrations tend to decrease and rubidium concentrations tend to increase. Consequently rubidium and strontium are negatively correlated, and the Rb/Sr ratio increases with increasing magma evolution.

Rubidium and strontium for all samples exhibit a significant negative correlation at the 99 percent confidence level (table 5). The average rubidium concentration and Rb/Sr ratio are lowest and the average strontium content is highest in the metaluminous granites (table 4). Thus, the peraluminous and peralkaline granites represent the most evolved magmas as is suggested by the REE data. This is shown graphically on figure 4. In general, the metaluminous granites contain more strontium and, in most cases, less rubidium than either the peraluminous or peralkaline granites.

The correlation between rubidium and strontium is better within individual plutons than it is for the entire data set and the specific relationship between rubidium and strontium varies slightly from pluton to pluton (fig. 4). By analogy, it seems likely that the correlation coefficients for the entire data set (table 5) are minimal and only indicative of general processes.

Correlation matrices for three groups of elements that exhibit good internal coherence are presented in table 6. The first matrix shows elements that are typically removed from a magma as a function of increasing degree of evolution (that is, compatible lithophile and siderophile elements). In addition to the elements shown in table 6, iron, manganese, and sodium also show a weak correlation with some of the compatible lithophile and siderophile elements, but the relationships are equivocal (table 5). Correlation analysis of the granites subdivided by degree of alumina saturation demonstrates that iron, manganese, and sodium are correlated with the compatible elements in the metaluminous granites but not in the more evolved peraluminous or peralkaline samples as shown by FeO and Na_2O (tables 7 to 9). Thus, from the correlation analysis and geochemical considerations, it is concluded that compatible lithophile and siderophile elements were separated early from the melt and that any economic concentrations of these elements would exist only at great depth. Economic potential for these elements is therefore considered to be low.

The last two groups of correlated elements given in table 6 are dominated by incompatible lithophile elements. These are typically enriched in granitic magmas with increasing degree of evolution. The two sets of incompatible lithophile elements are well correlated for both the entire data set (table 6) and for subsets based on degree of alumina saturation (tables 7 to 9). Rubidium, and to a lesser extent zirconium, are not well correlated with their covarying elements in the peralkaline and peraluminous subsets, respectively. These changes in correlation probably relate to late-stage effects, which are different in the two types of evolved magma.

Table 5.--*Partial correlation matrix for chemical data of postorogenic granites from the northeastern Arabian Shield*
[Major-element, uranium, and thorium data from Stuckless and others, 1982. Total iron as FeO. Oxide data treated arithmetically, elemental data treated logarithmically]

	SiO_2	Al_2O_3	FeO	MgO	CaO	Na_2O	K_2O	TiO_2	Ta	U	Th	Sr	Zr	La	Nd	Eu	Tb	Yb	Co
SiO_2		-0.70	-0.68	-0.80	-0.84	-0.67	-0.05	-0.88	0.38	0.40	0.43	-0.70	-0.17	-0.14	-0.18	-0.67	0.20	0.34	-0.55
Al_2O_3			0.07	0.59	0.68	0.51	0.26	0.53	-0.45	-0.35	-0.35	0.72	-0.33	-0.35	-0.42	0.23	-0.59	-0.46	0.69
FeO				0.59	0.53	0.53	-0.20	0.77	-0.18	-0.32	-0.35	0.32	0.63	0.33	0.48	0.60	0.27	0.00	0.01
MgO					0.92	0.44	-0.38	0.91	-0.54	-0.34	-0.34	0.64	-0.05	-0.10	-0.12	0.49	-0.41	-0.40	0.80
CaO						0.42	-0.17	0.88	-0.18	-0.27	-0.30	0.68	-0.04	-0.04	-0.05	0.32	-0.15	-0.08	0.53
Na_2O							-0.12	0.57	-0.36	-0.44	-0.48	0.45	0.22	0.02	0.13	0.53	-0.12	-0.30	0.35
K_2O								-0.16	-0.38	-0.04	0.04	0.09	-0.09	-0.04	-0.13	0.32	-0.46	-0.42	0.44
TiO_2									-0.37	-0.44	-0.47	0.62	0.22	0.36	0.44	0.84	0.00	-0.25	0.45
MnO	-0.67	0.21	0.79	0.53	0.55	0.54	-0.22	0.72	0.01	-0.30	-0.37	0.37	0.27	0.41	0.54	0.59	0.39	0.16	0.03
Ta										0.81	0.77	-0.44	0.17	0.38	0.30	-0.49	0.59	0.67	-0.49
U											0.89	-0.37	0.11	0.23	0.18	-0.57	0.53	0.66	-0.40
Th												-0.40	0.03	0.28	0.22	-0.58	0.52	0.62	-0.38
Rb	0.49	-0.39	-0.37	-0.43	-0.36	-0.50	0.07	-0.54	0.55	0.75	0.77	-0.49	-0.11	-0.25	-0.23	-0.66	0.34	0.61	-0.49
Sr													-0.11	-0.01	-0.05	0.65	-0.43	-0.46	0.78
Zr														0.61	0.75	0.48	0.56	0.27	-0.19
La															0.95	0.32	0.60	0.30	-0.09
Ce	-0.15	-0.36	0.37	-0.11	-0.03	0.04	-0.06	0.38	0.36	0.23	0.27	-0.02	0.66	0.99	0.97	0.35	0.65	0.34	-0.10
Nd																0.42	0.72	0.38	-0.14
Sm	-0.04	-0.53	0.44	-0.25	-0.10	0.05	-0.28	0.29	0.42	0.31	0.34	-0.23	0.73	0.86	0.95	0.25	0.88	0.60	-0.32
Eu																	-0.06	-0.32	0.47
Gd	0.13	-0.58	0.34	-0.40	-0.14	-0.05	-0.42	0.10	0.52	0.45	0.45	-0.38	0.64	0.68	0.81	0.04	0.98	0.80	-0.49
Tb																		0.88	-0.54
Dy	0.27	-0.58	0.20	-0.43	-0.15	-0.17	-0.48	-0.09	0.62	0.59	0.56	-0.46	0.48	0.52	0.63	-0.15	0.99	0.93	-0.59
Tm	0.33	-0.50	0.05	-0.42	-0.11	-0.27	-0.44	-0.22	0.68	0.66	0.62	-0.47	0.32	0.36	0.45	-0.29	0.92	0.99	-0.62
Yb																			-0.61
Lu	0.33	-0.42	-0.02	-0.38	-0.05	-0.32	-0.39	-0.26	0.66	0.65	0.61	-0.45	0.24	0.25	0.34	-0.33	0.85	0.99	-0.60
Hf	-0.19	-0.45	0.63	-0.18	-0.16	0.30	-0.32	0.34	0.43	0.33	0.30	-0.26	0.92	0.71	0.77	0.23	0.63	0.35	-0.28
Sc	-0.62	0.73	0.08	0.70	0.71	0.25	0.51	0.57	-0.47	-0.45	-0.47	0.87	-0.12	-0.15	-0.13	-0.33	-0.36	-0.32	0.69
Cs	0.10	0.41	-0.39	0.09	0.22	-0.06	0.09	-0.26	0.03	0.12	-0.01	0.17	-0.48	-0.49	0.47	-0.19	-0.10	0.23	0.09

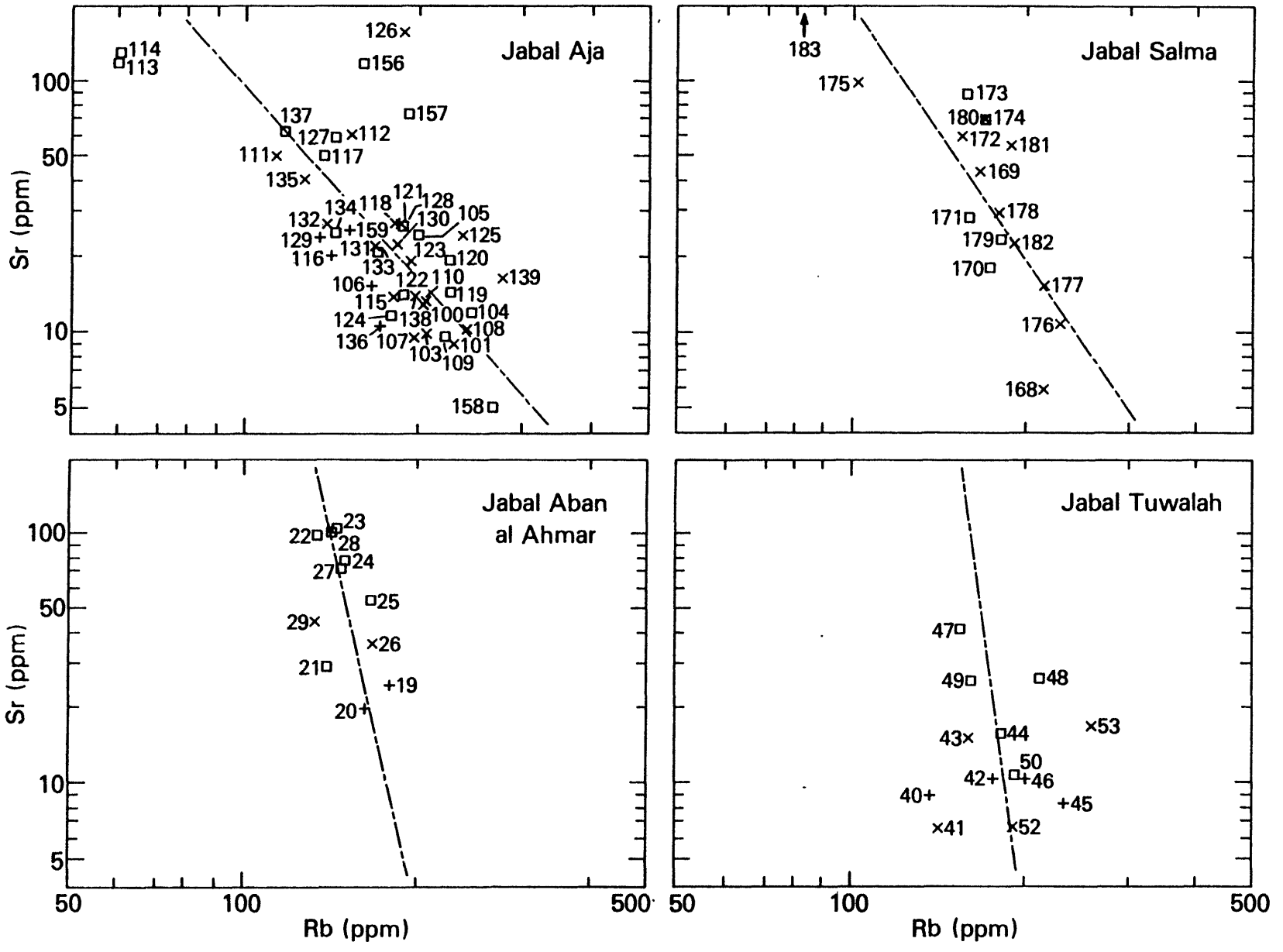

Figure 4.--Log-log plots of strontium (Sr) versus rubidium (Rb) concentrations, in parts per million (ppm), for samples from eight postorogenic plutons in the northeastern Arabian Shield. Symbols designate degree of alumina saturation: X, peraluminous; square, metaluminous; plus peralkaline. All sample numbers prefixed by 155; sample descriptions and locations in Stuckless and others, 1982.

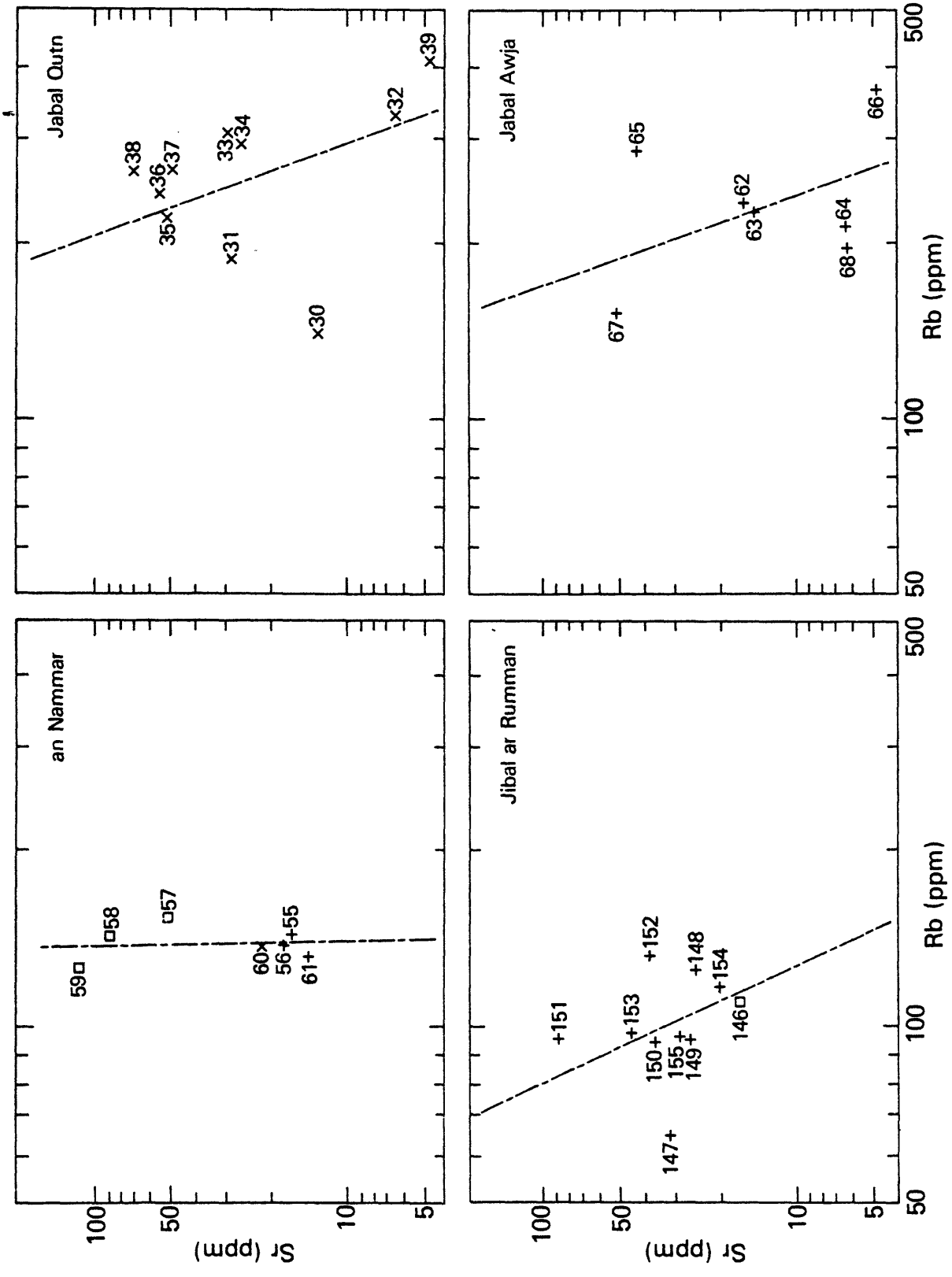

Figure 4.--Continued.

Table 6.--*Correlation matrices for selected sets of elements in postorogenic granites from the northeastern Arabian Shield*
[Oxide data treated arithmetically; elemental data treated logarithmically. Numbers below the diagonal line indicate number of samples used in correlation analysis]

	Al_2O_3	MgO	CaO	TiO_2	Sr	Sc	Co
Al_2O_3		0.59	0.68	0.53	0.72	0.73	0.69
MgO	176		.92	.91	.64	.70	.80
CaO	176	176		.88	.68	.71	.53
TiO_2	176	176	176		.62	.57	.45
Sr	175	175	175	175		.87	.78
Sc	72	72	72	72	71		.69
Co	72	72	72	72	71	72	

	Rb	U	Th	Yb	Lu	Ta
Rb		0.75	0.77	0.61	0.62	0.55
U	176		.89	.66	.65	.81
Th	176	176		.62	.61	.77
Yb	72	72	72		.99	.67
Lu	72	72	72	72		.66
Ta	72	72	72	72	72	

	La	Ce	Zr	Hf
La		0.99	0.61	0.71
Ce	72		.66	.73
Zr	72	72		.92
Hf	71	71	71	

Table 7.--*Correlation matrices for selected sets of elements in peraluminous granites from the northeastern Arabian Shield*
[Oxide data treated arithmetically; elemental data treated logarithmically. Numbers below the diagonal line indicate number of samples used in correlation analysis]

	Al_2O_3	MgO	CaO	TiO_2	Sr	Sc	Co	FeO	Na_2O
Al_2O_3		0.61	0.58	0.71	0.68	0.74	0.48	0.07	0.62
MgO	46		.62	.67	.80	.63	.85	.10	.36
CaO	70	46		.35	.61	.43	.15	-0.12	.14
TiO_2	70	46	70		.68	.48	.67	.57	.51
Sr	69	45	69	69		.80	.82	.13	.37
Sc	33	20	33	33	32		.62	.19	.27
Co	33	20	33	33	32	33		.46	.20
FeO	70	46	70	69	69	33	33		.17
Na_2O	70	46	70	70	69	33	33	70	

	Rb	U	Th	Yb	Lu	Ta
Rb		0.79	0.81	0.73	0.75	0.61
U	70		.88	.63	.62	.76
Th	70	70		.49	.48	.76
Yb	33	33	33		1.00	.55
Lu	33	33	33	33		.53
Ta	33	33	33	33	33	

	La	Ce	Zr	Hf
La		0.99	0.43	0.67
Ce	33		.42	.64
Zr	33	33		.78
Hf	32	32	32	

Table 8.--*Correlation matrices for selected sets of elements in metaluminous granites from the northeastern Arabian Shield*
[Oxide data treated arithmetically; elemental data treated logarithmically. Numbers below the diagonal line indicate number of samples used in correlation analysis]

	Al_2O_3	MgO	CaO	TiO_2	Sr	Sc	Co	FeO	Na_2O
Al_2O_3		0.67	0.78	0.74	0.81	0.75	0.80	0.64	0.84
MgO	49		.96	.97	.69	.78	.84	.86	.49
CaO	65	49		.97	.73	.84	.60	.87	.56
TiO_2	65	49	65		.72	.92	.62	.92	.56
Sr	65	49	65	65		.90	.69	.70	.65
Sc	25	16	25	25	25		.64	.79	.48
Co	25	16	25	25	25	25		.44	.67
FeO	65	49	65	65	65	25	25		.62
Na_2O	65	49	65	65	65	25	25	65	

	Rb	U	Th	Yb	Lu	Ta
Rb		0.81	0.81	0.66	0.64	0.69
U	65		.88	.76	.75	.81
Th	65	65		.82	.80	.75
Yb	25	25	25		1.00	.86
Lu	25	25	25	25		.86
Ta	25	25	25	25	25	

	La	Ce	Zr	Hf
La		0.99	0.76	0.78
Ce	25		.83	.81
Zr	25	25		.83
Hf	25	25	25	

Table 9.--*Correlation matrices for selected sets of elements in peralkaline granites from the northeastern Arabian Shield*
[Oxide data treated arithmetically; elemental data treated logarithmically. Numbers below the diagonal line indicate number of samples used in correlation analysis]

	Al_2O_3	MgO	CaO	TiO_2	Sr	Sc	Co	FeO	Na_2O
Al_2O_3		0.75	0.49	0.39	0.48	0.72	0.70	-0.52	0.80
MgO	30		.49	.52	.57	.61	.61	-0.26	.82
CaO	41	30		.74	.76	.80	.71	.19	.47
TiO_2	41	30	41		.76	.53	.38	.33	.45
Sr	41	30	41	41		.88	.67	.04	.41
Sc	14	8	14	14	14		.87	-0.38	.26
Co	14	8	14	14	14	14		-0.13	.52
FeO	41	30	41	41	41	14	14		.23
Na_2O	41	30	41	41	41	14	14	41	

	Rb	U	Th	Yb	Lu	Ta
Rb		0.59	0.64	0.06	0.03	-0.05
U	41		.90	.91	.91	.90
Th	41	41		.89	.88	.84
Yb	14	14	14		.99	.91
Lu	14	14	14	14		.89
Ta	14	14	14	14	14	

	La	Ce	Zr	Hf
La		1.00	0.70	0.64
Ce	14		.71	.66
Zr	14	14		.98
Hf	14	14	14	

For example, alkali complexing with volatiles that have been removed from the peralkaline magma may result in a rubidium depletion rather than continued enrichment with increasing magma evolution. Similarly, attainment of a saturation limit for zirconium in the peraluminous magma may prevent continued enrichment of zirconium with increasing degree of evolution for these magmas.

The combined evidence for substantial enrichment with magma evolution and the occurrence of a few of these elements in some late-stage segregates and pegmatites (Delfour, 1977; Stuckless and others, unpub. data) suggests that there is some economic potential for pegmatite or veins that contain uranium, thorium, rare-earth elements, tantalum, and presumably niobium. The greatest enrichment of these elements and the best internal covariation are noted for the peralkaline granites. Subeconomic occurrences for this suite of elements have already been reported in the Midian Mountains (Harris and Marriner, 1980). It therefore seems likely that more occurrences of this type and possibly ones of economic quality can be located in association with peralkaline plutons.

SUMMARY AND CONCLUSIONS

All trace-element concentrations obtained for the postorogenic granites in this study are best described by lognormal statistics. Variations in key petrologic indicators, such as rubidium and strontium contents and europium anomalies, show that metaluminous granites are least evolved and that peralkaline and peraluminous granites are most evolved. Correlation analysis shows that the more evolved granites are enriched in one of two suites of internally correlated trace elements, all of which can be classified as incompatible lithophile elements. The less evolved granites contain a suite of internally correlated compatible lithophile or siderophile trace elements. It is concluded that there may be economic potential for the suites of incompatible elements (uranium, thorium, REE, tantalum, and presumably niobium) in the form of vein or pegmatitic deposits. Available data indicate that the compatible trace elements were removed from the magma during the early stages of differentiation and that therefore any economic concentration of these elements would exist only at inaccessible depths.

The trace-element data show that all postorogenic granites sampled in the current study, except the granite at Jabal Qutn, belong to the zirconium-niobium group of specialized granites as defined by Elliott (unpub. data, 1982). The area from which these granites were collected corresponds to the region in which the protolith for the igneous rocks has isotopic affinities to an oceanic crust (J. S. Stacey and D. B. Stoeser, written commun., 1982). Thus a protolithic control

is suggested for the various types of specialized granites, and although tin and tungsten data are unavailable, the probability of anomalous concentrations of these elements, as reported to the southeast at Baid al Jimalah (Cole and others, 1981), seems low. The somewhat different trace-element systematics for samples from Jabal Qutn may represent a transition from one type of specialized granite to another.

The geologic processes noted in association with anomalous concentrations of zirconium and other trace elements within the study area suggest that the action of volatile elements may be important in the formation of ore deposits in this region. Because volatile saturation toward the end stage of magmatism is suggested by presumed volcanic equivalents of the postorogenic granites, vein and pegmatitic deposits are the most likely targets for economic concentrations of trace elements.

Simpson and others (1982) have recently proposed a model for enrichment of volatiles in granitic magmas and consequent formation of ore deposits. The model is based on addition of water from the intruded country rocks. The additional water increases the probability of forming both late-stage magmatic and secondary vein deposits. On the basis of this model, it is recommended that the best targets for future exploration are areas in which highly evolved peralkaline or peraluminous plutons intruded hydrous metasedimentary rocks.

REFERENCES CITED

Anderson, J. L., and Cullers, R. L., 1978, Geochemistry and evolution of the Wolf River Batholith, a late Precambrian rapakivi massif in North Wisconsin, USA: Precambrian Research, v. 7, p. 287-324.

Anderson, J. J., Cullers, R. L., and Van Schmus, W. R., 1980, Anorogenic metaluminous and peraluminous granite plutonism in the mid-Proterozoic of Wisconsin, USA: Contributions to Mineralogy and Petrology, v. 74, p. 311-328.

Anderson, J. L., *in press*, Proterozoic anorogenic granite plutonism of North America: Geological Society of America Memoir.

Arth, J. G., and Hanson, G. N., 1972, Quartz diorites derived by partial melting of eclogite or amphibolite at mantle depths: Contributions to Mineralogy and Petrology, v. 37, p. 161-174.

Arth, J. G., and Hanson, G. N., 1975, Geochemistry and origin of the early Precambrian crust of northeastern Minnesota: Geochimica et Cosmochimica Acta, v. 39, p. 325-362.

Barker, F., Millard, H. T., Jr., Hedge, C. E., and O'Neil, J. R., 1976, Pikes Peak batholith; geochemistry of some minor elements and isotopes, and implications for magma genesis: in Epis, R. C., and Weimer, R. J., eds., Professional Contributions of Colorado School of Mines, no. 8, p. 44-56.

Bowden, P., and Kinnaird, J. A., 1978, Younger granites of Nigeria; a zinc-rich tin province: Transactions of the Institute of Mining and Metallurgy, v. 87, p. B66-B69.

Buma, Grant, Frey, F. A., and Wones, D. R., 1971, New England granites: Trace element evidence regarding their origin and differentiation: Contributions to Mineralogy and Petrology, v. 31, p. 300-320.

Christiansen, E. H., Bikus, J. V., Sheridan, M. F., and Burt, D. M., *in press*, Geochemical evolution of topaz rhyolites from the Thomas Range and Spor Mountain, Utah: Contributions to Mineralogy and Petrology.

Christiansen, E. H., Burt, D. M., Sheridan, M. F., and Wilson, R. T., *in press*, The petrogenesis of topaz rhyolites from the western United States: Contributions to Mineralogy and Petrology.

Cole, J. C., Smith, C. W., and Fenton, M. D., 1981, Preliminary investigation of the Baid al Jimalah tungsten deposit, Kingdom of Saudi Arabia: U.S. Geological Survey Open-File Report 81-1223, (IR)SA-377, 26 p.

Cullers, R. L., Koch, R. J., and Bickford, M. E., 1981, Chemical evolution of magmas in the Proterozoic terrane of the St. Francois Mountains, southeastern Missouri, Part 2, Trace element data: Journal of Geophysical Research, v. 86, p. 10388-10401.

Delfour, J., 1977, Geology of the Nuqrah quadrangle, sheet 25E, Kingdom of Saudi Arabia: Saudi Arabian Directorate General of Mineral Resources Geologic Map GM-28, 32 p., scale 1:250,000.

Doe, B. R., Stuckless, J. S., and Delevaux, M. H., 1982, The possible bearing of the granite of the UPH deep drill holes, northern Illinois, on the origin of Mississippi Valley ore deposits: American Geophysical Union Memograph [in press].

Evensen, N. M., Hamilton, P. J., and O'Nions, R. K., 1978, Rare-earth abundances in chondritic meteorites: Geochimica et Cosmochimica Acta, v. 42, p. 1199-1212.

Frey, F. A., Chappell, B. W., and Roy, S. D., 1978, Fractionation of rare-earth elements in the Tuolumne Intrusive Series, Sierra Nevada Batholith, California: Geology, v. 6, p. 239-242.

Gordon, G. E., Randle, Keith, Goles, G. G., Corliss, J., Beeson, M., and Oxley, S., 1968, Instrumental activation analysis of standard rocks with high resolution gamma ray detectors: Geochimica et Cosmochimica Acta, v. 32, p. 369-396.

Hanson, G. N., 1978, The application of trace elements to the petrogenesis of igneous rocks of granite composition: in Allegre, C. J., ed., Trace elements in igneous petrology, Earth and Planetary Science Letters, v. 38, p. 26-43.

Harris, N. B. W., and Marriner, G. F., 1980, Geochemistry and petrogenesis of a peralkaline granite complex from the Midian Mountains, Saudi Arabia: Lithos, v. 13, p. 325-337.

Kinnaird, J., Bowden, P., and Whitley, J. E., 1982, Uranium mineralization in an anorogenic setting in Nigeria (abs.): Unpublished report to IAEA/NEA Joint R & D project 6.

Naney, M. T., and Swanson, S. E., 1980, The effect of Fe and Mg on crystallization in granitic systems: American Mineralogist, v. 65, p. 639-653.

Radain, A. A. M., Fyfe, W. S., and Kerrich, R., 1981, Origin of peralkaline granites of Saudi Arabia: Contributions to Mineralogy and Petrology, v. 78, p. 358-366.

Shand, S. J., 1951, Eruptive rocks: New York, John Wiley, 488 p.

Simpson, P. R., Plant, J. A., Watson, J. V., Green, P. M., and Fowler, M. B., 1982, The role of metalliferous and mineralized uranium granites in the formation of uranium provinces: Symposium on uranium exploration methods, NEA/IAEA R & D Program, Paris, France, 12 p.

Stacey, J. S., Doe, B. R., Roberts, R. J., Delevaux, M. H., and Gramlich, J. W., 1980, A lead isotope study of mineralization in the Saudi Arabian Shield: Contributions to Mineralogy and Petrology, v. 74, p. 175-188.

Streckeisen, A. L., 1973, Plutonic rocks, classification and nomenclature recommeded by the IUGS Subcommission on the Systematics of Igneous Rocks: Geotimes, v. 18, p. 26-30.

Stuckless, J. S., and Miesch, A. T., 1981, Petrogenetic modeling of a potential uranium source rock, Granite Mountains, Wyoming: U.S. Geological Survey Professional Paper no. 1225, 39 p.

Sun, S. S., and Hanson, G. N., 1976, Rare earth element evidence for differentiation of McMurdo volcanics, Ross Island, Antarctica: Contributions to Mineralogy and Petrology, v. 54, p. 139-155.

Taylor, R. P., Strong, D. F., and Kean, B. F., 1980, The Topsails igneous complex; Silurian-Devonian peralkaline magmatism in western Newfoundland: Canada Journal of Earth Sciences, v. 17, p. 425-439.

VanTrump, George, Jr., and Miesch, A. T., 1977, The U.S. Geological Survey RASS-STATPAC system for management and statistical reduction of geochemical data: Computer and Geosciences, v. 3, p. 475-488.

Watson, E. B., 1979, Zircon saturation in felsic liquids: Experimental results and applications to trace element geochemistry: Contributions to Mineralogy and Petrology, v. 70, p. 407-419.

Watson, J., Fowler, M. B., Plant, J., Simpson, P. R., and Green, P. M., 1982, Uranium provinces in relation to metamorphic grade and regional geochemistry: Symposium on uranium exploration methods, NEA/IAEA R & D Program, Paris, France, 11 p.

Wilson, M. R., and Åkerblom, G., 1980, Uranium enriched granites in Sweden: Sveriges Geologiska Undersokning Rapporter och Meddelanden, v. 19, Uppsala, 30 p.

York, Derek, 1969, Least-squares fitting of a straight line with correlated errors: Earth and Planetary Science Letters, v. 5, p. 320-324.